Fuzzy Based AC-DC-AC Converter Controlled Micro Hydro Renewable Power Generation using Parallel Asynchronous Generators for Remote Areas

P. Devachandra Singh*‡, Sarsing Gao**

*Department of Electrical Engineering, Assistant Professor, North Eastern Regional Institute of Science and Technology, Nirjuli, Arunachal Pradesh, India-791109

**Department of Electrical Engineering, Professor, North Eastern Regional Institute of Science and Technology, Nirjuli, Arunachal Pradesh, India-791109

(ptombel@gmail.com, sg@nerist.ac.in)

‡ P. Devachandra Singh, Department of Electrical Engineering, Assistant Professor, North Eastern Regional Institute of Science and Technology, Nirjuli, Arunachal Pradesh, India-791109, ptombel@gmail.com

Received: 06.02.2020 Accepted:03.03.2020

Abstract- A new micro hydro power generation (MHPG) scheme is proposed for supplying loads located at remote areas far away from grid. This paper presents three major contributions for small scale renewable hydro power generation technology. Firstly, the proposed model uses unregulated flow rates for two different generators for generating small scale hydroelectricity which otherwise generally uses constant flow rates. Secondly, a new architecture of converter is designed and implemented for parallel operation of two variable speed generators. Thirdly, a fuzzy PI based converter control is designed for the proposed MHPG system, which is found to perform better than that of conventional PI control based systems. In this, a new architecture of AC-DC-AC converter is used for controlling two parallel operated variable speed Capacitor Excited Asynchronous Generators (CAGs). The two CAGs are considered to be operated at variable speeds as fed by two different variable turbines. The converter system consists of two numbers of two level voltage source converters (VSCs) and one common voltage source inverter (VSI). The control algorithms are appropriately designed so as to manage the variable inputs by converting each of the generated variable ac voltages to dc voltage at a common dc bus. The VSI provides constant voltage and frequency at the load end. This architecture eliminates the problem of synchronization of two variable sources and also optimizes the cost and components required compared to that of system using individual back to back converters for each generating units. The proposed scheme is investigated and analysed to assess the feasibility in terms of its performance and quality of power under different loads such as resistive and inductive loads. Firstly, the switching frequency and modulation index for the converter are determined for giving efficient performance. Finally, the performance of the proposed fuzzy PI controlled converter based MHPG and that of conventional PI controlled converter system is compared and presented. The modeling and the simulation are carried out in MATLAB/Simulink environment.

Keywords Micro Hydro Power Generation, AC-DC-AC Converter, Fuzzy PI Controller, Parallel Asynchronous Generators.

1. Introduction

The carbon emissions and environmental degradations due to conventional electricity generations poses a global concern and need to be addressed at utmost priority. The World Energy Forum predicts the fossil fuel reserves will be exhausted in less than another 10 decades [1]. Therefore, there is urgent need to arrest the climatic changes before it goes to a catastrophic condition. Efforts must be made to increase the penetration of renewable energy into the utility grid. A global target has been set to increase the renewable energy generation to 4550 GW by 2040 from 1700 GW in 2014 by the International Energy Agency's Word Energy Forum [1]. The contribution from renewable energy sources (RES) is about 26.5% as in 2017 and of which 61.9% comes from hydro power [2]. This contribution is reduced compared

to 83% in 2014 due to small increment in electricity generated from hydropower compared to fast growth of wind energy [3]. India has a total potential of renewable energy of about 8,96,602 MW of which 7,48,991 MW is from solar power, 1,02,772 MW is from wind energy, 19,749 MW is from small hydro power and 25,090 MW is from bio-energy as per the estimate given by Ministry of New and Renewable Energy Sources(MNRES) [3]. The installed capacity of small hydro power generation (SHPG) is only 4,379.86 MW till the end of March 2017 contributing only 7.17% of the total renewable energy installed capacity in India. To increase the contribution from hydro power, this work closely looks into the sustainability and technological development in the area of small scale hydro power electricity generation, especially in the Himalayan regions or any geographical region where the potential of small scale hydro power electricity generation is significant.

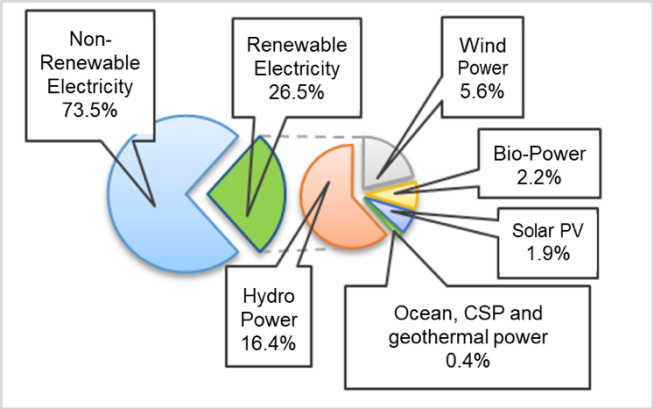

Fig. 1. Renewable energy contribution in global electricity production [2].

The conventional SHPG consists of mainly synchronous generators which require constant speed operation imposing properly designed civil construction in the stream near inlet to the turbine of the generator. Broadly, hydro power can be classified into five categories based on the type of installation, which are; impoundment type (suitable for large system using dam), diversion type, pump storage and run off river (natural free flowing water of river) type [4]. This study is focussed mainly for hydropower system with run off river. Hence, the application of simple CAG is investigated for the purpose of extracting power from free flowing stream of river water. The CAG has many advantages such as low cost and maintenance, simple and robust construction, etc. It also has inherent capability to operate at variable speeds and ability to handle any type of load [5]. Besides, it has the advantage as it provides natural protection against short circuit fault and also it is better than PMSG at medium speed operation [6]. In this study, the CAG is considered for variable speed operation as the flow is uncontrolled and thus, the turbines run at variable speeds. To facilitate efficient extraction of electricity from such streams, implementation of an active front end converter is proposed. Many works are reported in the proposed model but mainly in the field of wind energy generation system (WEGS) and very few for SHPG [7-9]. Some studies have presented use of controllers like static VAR compensator, neural network technique for controlling output voltage of CAG fed by variable prime mover but the frequency is not regulated at rated value [10, 11]. The active front end converter in SHPG can provide constant output frequency and offer more flexibility in power flow control thereby improving its efficiency. The harmonics injected due to use of converter can be reduced by adjusting the values of modulation index and switching frequency [12]. Further, the necessity of the gear box arrangement for wind energy applications is not required in case of SHPG where the variation of flow rate is comparatively small. There are many topologies applied to DFIG, PMSG, etc., which are popular where the wind variation is very large and highly unpredictable [5-15]. This paper emphasizes on designing a simple and comparatively efficient and convenient system for extracting electricity from free flowing streams.

The proposed scheme uses two CAGs in parallel to extract maximum potential of such energy sources as shown in Fig.2. The study of parallel operation of CAGs is started about more than two decades ago [16-19]. The parallel operated CAGs has numerous advantages as it does not require synchronization and reduced hunting problems due to higher damping, etc. [16, 18]. However, the CAGs should be connected in proper phase sequence to avoid instability of the system [17]. The investigation on parallel operation of CAGs are also found to study with variation in rotor parameters [19]. Another literature presents the parallel operation based on constant turbine inputs [20]. The study of a hybrid parallel operation of synchronous and induction generators is also presented [21]. The proposed topology has added advantages in terms of easy parallel operation, possibility of synchronization with main grid, lesser components requirements compared to individual sets of AC-DC-AC converters for each machines; it has a superior control as compared to other topologies. These advantages are envisaged to compensate extra cost required for additional AC-DC converter units.

The conventional PI controller is widely used technique for the control of the converter. However, in this paper, the fuzzy logic based controller is designed and implemented. Controllers using soft computing techniques like fuzzy logic, artificial neural network, genetic algorithms, hybrid neuro fuzzy etc. are prevailing in the present times [22, 23]. The fuzzy based system is found to be superior compared to conventional controllers in many cases [8, 9, 13, 22-29]. Application of fuzzy control strategy is presented where the grid side control of a PMSG based wind generation system uses Takagi-Sugeno fuzzy control system to maintain the dc link voltage of an AC-DC-AC converter [9, 13]. A complete fuzzy control based WEGS is presented in yet another study where the control objectives are mainly optimization of efficiency and enhancement of performances [8]. The advantages of squirrel cage induction machine as generator for WEGS with improved dynamic performances with the use of fuzzy logic control principle is detailed in [25]. In yet another study, fuzzy based controller shows better performances compared to that of a conventional PI controller in controlling active and reactive power for improved stability and power quality of a DG (Distributed

Generator) system connected to utility grid [28]. In all the studies, fuzzy control gives advantages such as parameter insensitivity, faster convergence, and acceptance of noisy and inaccurate signals when applied to wind energy conversion system.

This paper presents three major contributions focussing on the technological development in the area of small scale hydro power generation. Firstly, the paper presents a novel MHPG system with unregulated flow rates applied to two different CAGs operating in parallel generating variable voltages and frequencies; the conventional MHPG systems generally use constant flow rates accomplished by costly civil works for flow control. Such studies are carried out on wind energy conversion systems and rather not on MHPG system. Secondly, a new converter architecture is designed and implemented for parallel operation of two variable speed generators. Thirdly, a fuzzy PI based converter control scheme is implemented with optimized modulation index and switching frequencies, which gives a two stage optimization solution to the overall system for efficient performance.

The feasibility study of the proposed model is carried out under three basic objectives. Firstly, the determination of the optimum values of switching frequency and the modulation index suitable for the proposed model. Secondly, the performance analysis of the proposed scheme with conventional PI control and fuzzy PI control under the optimum condition. In both the cases, the MHPG system is being operated in isolated mode supplying two different types of load viz. resistive and inductive loads. Thirdly, the comparison of the performances of the above systems.

2. Description of the proposed system

The schematic diagram of the proposed system is illustrated in Fig. 2. Two numbers of CAGs are used to operate in variable speed modes without regulating in the generator circuit. As CAG requires reactive power for its operation and maintaining the terminal rated voltage at rated speed, a capacitor bank is used for each of the CAGs as shown in Fig.3. The saturation parameters required for the simulation are obtained from the open circuit test of the machines. The proposed MHPG system in this paper consists of variable water turbines coupled to each CAGs, which is connected to the consumer load by means of an IGBT based active front end converter. Both the rectifier and the inverter in the converter are controllable and control is achieved by complementary switching functions which define the conversions between the DC and AC buses. The CAG obtains its reactive power from a star configured excitation capacitor bank which helps the machine to generate rated terminal voltage at rated speed of the machine. The saturation parameters are experimentally obtained from the no-load test of the machine. However, since the hydro turbine operates at variable speed, the output voltage and frequency are deviated from the rated values. These deviations are further extended under variation in load. The additional reactive power required for regulation of these variations are supplied by dc link capacitance. The control algorithms of the generator side and load side converters are discussed in the subsequent sections. The approximate variation of the water turbine is taken as per the expected range of variations in a small river in terms of flow rate measured in cubic metre per sec (m^3/sec). However, the variation is comparatively small as compared to that of wind turbine. The modelling of the turbine is carried out by determining the torque-speed characteristics with respect to changing flow rate. The mechanical output power (P_m) of the

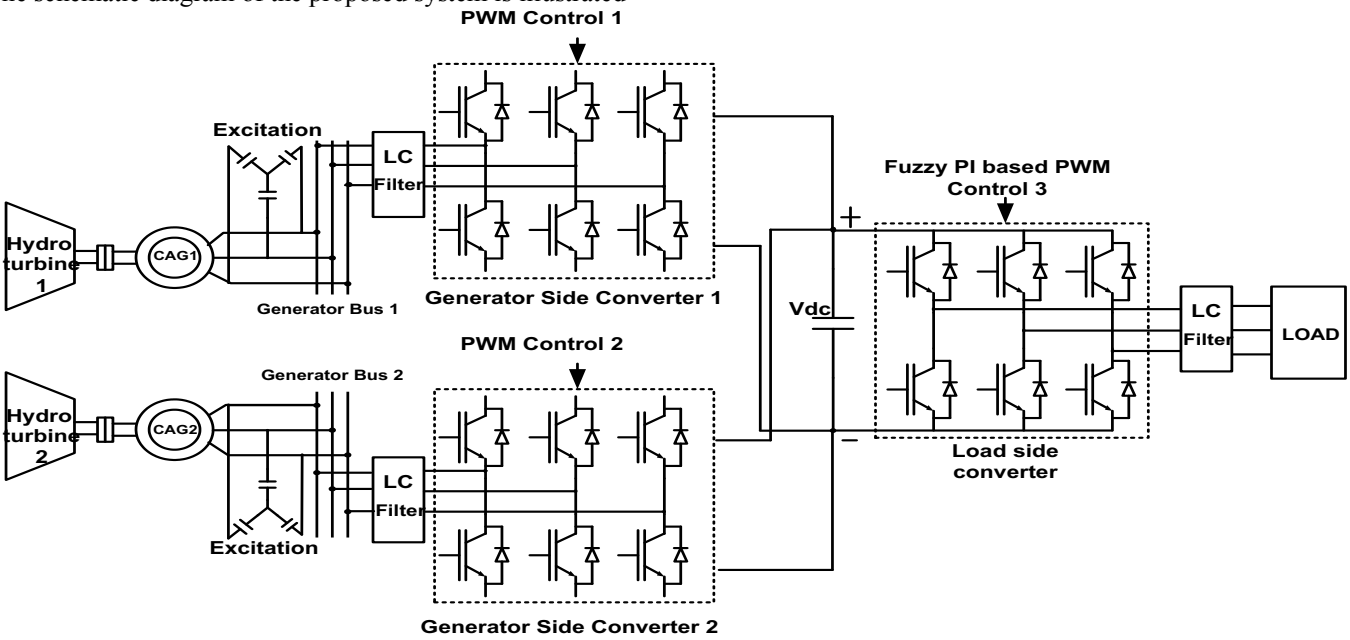

Fig. 2. Schematic diagram of the proposed MHPG scheme.

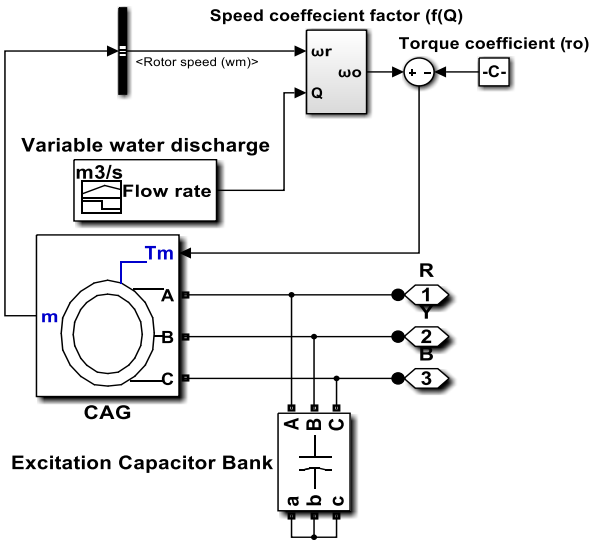

Fig. 3. CAG model along with excitation capacitor and turbine.

variable speed prime mover with rotor speed, ω_r rad/sec and mechanical torque, T_m N.m is given by mechanical torque

$$P_m = T_m \omega_r \tag{1}$$

Where, T_m can be expressed in terms of torque coefficient (τ_0) and speed coefficient (n_0) as

$$T_m = \tau_0 - n_0 \frac{\omega_r}{\omega_s} \tag{2}$$

$$T_m = \tau_0 - \omega_0 \omega_r \tag{3}$$

Where, $\omega_0 = n_0 / \omega_s$ and ω_0 and ω_s are the angular speed coefficient and angular synchronous speed in rad/sec.

In this paper, run of the river scheme is investigated, hence, the mechanical output power (P_m) can be given by

$$P_m = \frac{1}{2} \eta \rho Q v^2 \tag{4}$$

Where, η, ρ, Q and v are the efficiency of turbine, density of water (kg/m^3), flow rate (m^3/sec) and velocity of water (m/sec).

From equations (1) and (4),

$$T_m = \frac{1}{2\omega_r} \eta \rho Q v^2 \tag{5}$$

In the equation (5), 'v' can also be expressed in term of 'Q' as $v = Q/A$, where 'A' is the swept area of the turbine blades in m^2. Hence, the variable turbine modelled with respect to varying 'Q'. From equations (3) and (4), by solving a quadratic equation of angular speed it can be determined that ω_0 is a function of flow rate (Q). Thus, equation (3) is re-written in equation (6) and the same is implemented in the turbine model shown in Fig. 3 above for obtaining the turbine torque-speed characteristics wrt to varying 'Q'.

$$T_m = \tau_0 - f(Q).\omega_r \tag{6}$$

3. Control Methodology

The basic algorithm of the controller of the proposed converter is based on the principle of de-coupling d-q components of currents and voltages in the generator and load/grid sides to maintain dc-link voltage, power factor and terminal voltage. The converter control algorithm is developed by decoupling d-q components of the corresponding three phase components. The generator side control maintains the dc link voltage at the dc bus while the load side converter control ensures constant voltage at load terminal. The d-component has control over active power while the q-component has control over the reactive power. Thus the control algorithms are developed so as to regulate these powers and the desired output are maintained. The transformation of three phase components to d-q-0 components are done with the help of Park's transformation and further converted back to three phase components after applying control techniques to each of d and q components. The following equations show the formulae for Park's transformation and Inverse's Park's transformation:

Park's transformation

$$V_{dq0} = K V_{abc} \tag{7}$$

Where,

$$V_{abc} = \begin{bmatrix} V_a \\ V_b \\ V_c \end{bmatrix}, \; V_{dq0} = \begin{bmatrix} V_d \\ V_q \\ V_0 \end{bmatrix} \tag{8}$$

$$K = \frac{2}{3} \begin{pmatrix} \cos\omega t & \cos\left(\omega t - \frac{2\pi}{3}\right) & \cos\left(\omega t + \frac{2\pi}{3}\right) \\ \sin(\omega t) & \sin\left(\omega t - \frac{2\pi}{3}\right) & \sin\left(\omega t + \frac{2\pi}{3}\right) \\ \frac{1}{2} & \frac{1}{2} & \frac{1}{2} \end{pmatrix} \tag{9}$$

Inverse Park's transformation

The Inverse Park's transformation is done as follows:

$$V_{abc} = K^{-1} V_{dq0} \tag{10}$$

Where,

$$K^{-1} = \begin{pmatrix} \cos\omega t & -\sin\omega t & 1 \\ \cos\left(\omega t - \frac{2\pi}{3}\right) & -\sin\left(\omega t - \frac{2\pi}{3}\right) & 1 \\ \cos\left(\omega t + \frac{2\pi}{3}\right) & -\sin\left(\omega t + \frac{2\pi}{3}\right) & 1 \end{pmatrix} \quad (11)$$

3.1. Generator side control (GSC)

The block diagram showing the control of generator side is given in Fig. 4. The main function of the generator side control is to maintain the dc link voltage to a reference value and unity power factor. Firstly, the system frequency is synchronized by using an internal oscillator based phase lock loop (PLL) from the three phase voltages measured in the generator side. The three phase components of measured voltages and currents are converted into dq0 components using Park's transformation as given in equation (13). The direct axis component of the measured current (i_d) is compared with the reference value of the current ($i_{d\text{-}ref}$) and regulated through a PI controller to give its controlled output as shown in equation (13). This reference current ($i_{d\text{-}ref}$) is obtained from controlled output of the comparison between the measured dc link voltage (V_{dc}) and the reference dc voltage ($V_{dc\text{-}ref}$) as shown in equation (12). The quadrature component of the current (i_q) is being passed through an offset controller to maintain unity power factor. The controlled output of both the direct and quadrature components are further regulated by a current regulator as

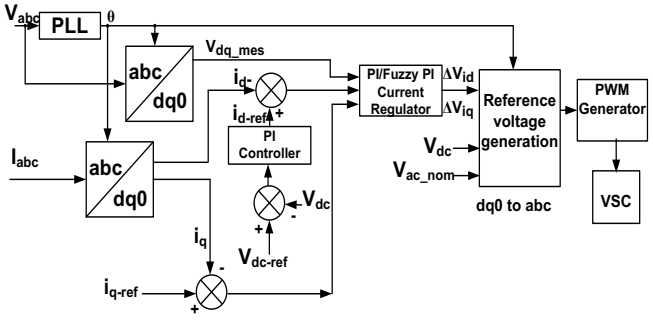

Fig. 4. Control scheme of generator side converter.

shown in equations (14) and (15). This current regulator implementing PI controller and Fuzzy PI controller are studied separately. The output of this regulator is fed to a reference voltage generation block to estimate the modulation index and the phasor angles to provide the required modulating signal at its output. Subsequently, the PWM generator gets its input modulating signal for generating gating pulses of the IGBTs based converter. The PWM uses a carrier frequency of 2 kHz.

DC voltage regulator:

$$I_{dref} = \left(K_p + \int K_i\right)\left(V_{dcref} - V_{dc}\right) \quad (12)$$

$$V_{dc} = \left(K_p + \int K_i\right)\left(I_d - I_{dref}\right) \quad (13)$$

Current Regulator:

$$V_{d\_mes} + I_d \times \mathrm{R} - I_q \times \omega L + \frac{dI_d}{dt} \times L = V_{d\_conv} \quad (14)$$

$$V_{q\_mes} + I_d \times \omega L + I_q \times R + \frac{dI_q}{dt} \times L = V_{q\_conv} \quad (15)$$

A generator side filter is used in the scheme to reduce the heating of the generator windings to some extent. The generator side harmonics consist of low frequency and high frequency harmonics generated from the variable speed generator and switching devices respectively. Such filter is usually found absent in many variable turbine wind energy systems as only the load side harmonics is given more emphasis. An LC filter is used for the purpose, where the harmonics generated from switching devices are taken care of.

3.2. Load side control (LSC)

This control ensures constant voltage at load terminal. It consists of discrete PLL device synchronized with 50 Hz frequency, abc to dq0 transformation unit, comparators, controllers including Fuzzy PI controllers, reference voltage generator and PWM generator as shown in Fig. 5. After transforming the measured load voltage into d-axis and q-axis components (V_d and V_q) and comparing with the respective references ($V_{d\text{-}ref}$ and $V_{q\text{-}ref}$), the error signals are regulated by PI controllers as given in equations (16) and (17). This control loop using fuzzy PI controller is discussed in Section 4. A discrete PLL unit synchronized at rated frequency provides sin-cos and the phase angle required by the other blocks. The reference voltage generator provides the modulating signal for the PWM generator to generate the required gating pulses of the load side converter. The working of the PI controllers for d-axis and q-axis components are given below:

$$V_d = \left(K_p + \int K_i\right)\left(V_{dref} - V_{dmes}\right) \quad (16)$$

$$V_q = \left(K_p + \int K_i\right)\left(V_{qref} - V_{qmes}\right) \quad (17)$$

In an IGBT/thyristor based voltage source converter, rated ac output voltage can be maintained by regulating the modulation index along with the voltage profile of dc link bus voltage given by the equation (18).

$$V_{Line} = \frac{m}{2}\sqrt{\frac{3}{2}}V_{dc} \quad (18)$$

To smoothen the inverted output voltage close to sinusoidal waveform, LC filter is connected at the inverter output terminals. The inductance, L and capacitance, C can be related as given below:

$$C\frac{d\overline{V}_{cap}}{dt} = \overline{I}_{invt} - \overline{I}_{ld} \tag{19}$$

$$L\frac{d\overline{i}_{invt}}{dt} = \overline{V}_{invt} - \overline{V}_{cap} \tag{20}$$

Where, $\overline{V}_{cap}$ is the voltage of capacitor filter, $\overline{V}_{invt}$ is output voltage of inverter, $\overline{I}_{invt}$ and $\overline{I}_{ld}$ are currents in the inverter and the load respectively.

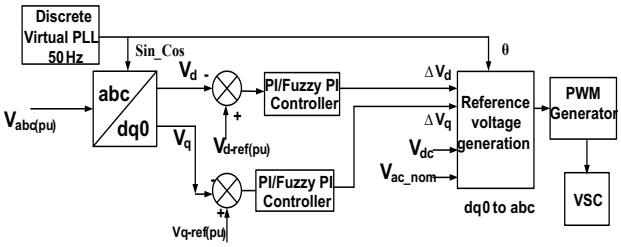

Fig. 5. Control scheme of converter at load side.

The respective equations for d-q axis components of the voltage are as follows:

$$\overline{V}_{q(cap)} = \frac{1}{C}i_{q(invt)} - \omega V_{d(cap)} - \frac{1}{C}i_{q(ld)} \tag{21}$$

$$\overline{V}_{d(cap)} = \frac{1}{C}i_{d(invt)} + \omega V_{q(cap)} - \frac{1}{C}i_{d(ld)} \tag{22}$$

$$i_{q(invt)} = \frac{1}{L}V_{q(invt)} - \omega i_{d(invt)} - \frac{1}{L}V_{q(cap)} \tag{23}$$

$$i_{d(invt)} = \frac{1}{L}V_{d(invt)} + \omega i_{q(invt)} - \frac{1}{L}V_{d(cap)} \tag{24}$$

Where $\omega = 2\pi f$ and 'f' is the frequency of the inverter ac voltage.

Considering an instantaneous load power from the input power to the dc link capacitor, the balanced power equation is given as [30]:

$$V_{dc}I_{dc} = \frac{3}{2}\left(v_{q(cap)}i_{q(ld)} + v_{d(cap)}i_{d(ld)}\right) \tag{25}$$

Where V_{dc} and I_{dc} are the dc link voltage and the current and I_{dc} are the dc link voltage and the current respectively.

4. Fuzzy logic controller

In the proposed fuzzy PI controller shown in Fig. 6(a), the error (e) and the change in error (Δe) are taken as the two inputs to the controller and the output is decided by the rule base look up table so developed as provided in Table 1. In fuzzy PI controller, fuzzy inference system is used to adapt the parameters of conventional PI controller which will improve the robustness and adaptability [31, 32]. The triangular membership functions are chosen for both input as well as output and the fuzzy inference system used is the most widely used Mamdani method. The fuzzy PI controllers so developed are implemented as shown in the control schemes of the generator side as well as load side converter as shown in Fig. 6 (b). The error computations are

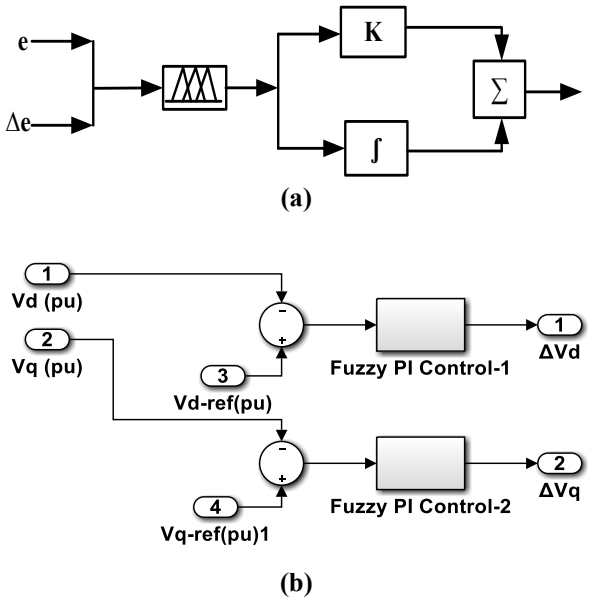

Fig. 6. (a) Fuzzy PI control structure applied to GSC and LSC (b) Fuzzy PI control structure.

carried out with pu values of measured voltage and current and hence the input and output ranges of the triangular membership functions are set in the range of -1 to 1 as shown in Fig 7 (a). Similar membership functions are applied to each of the GSCs and LSC except Vd and Vq in Fig. 6(b) are rather Iq and Iq respectively in the case of LSC. Hence, six FIS programs are developed using IF-THEN Mamdani rule as per Table 1, such as "gsc1d.fis" and "gsc1q.fis" are for each of Vd and Vq of GSC-1 respectively. In the same manner, "gsc2d.fis" and "gsc2q.fis" are developed for GSC-2 and "lscd.fis" and "lscq.fis" for LSC. An IF-THEN rule implementation and surface representation of the rule are illustrated in Fig. 7 (b) and (c) respectively. The output of the fuzzy PI controllers are obtained by applying centroid method of defuzzification. Accordingly, the regulated outputs of the direct axis and quadrature axis components given in the equations (16) and (17) will be obtained as per the control logic of fuzzy PI controller and these outputs are subsequently fed to the reference voltage generator.

Table 1. Fuzzy Rule Base

e \ Δe	NB	NM	NS	Z	PS	PM	PB
NB	NB	NB	NB	NB	NM	NS	Z
NM	NB	NB	NB	NM	NS	Z	PS
NS	NB	NB	NM	NS	Z	PS	PM
Z	NB	NM	NS	Z	PS	PM	PB
PS	NM	NS	Z	PS	PM	PB	PB
PM	NS	Z	PS	PM	PB	PB	PB
PB	Z	PS	PM	PB	PB	PB	PB

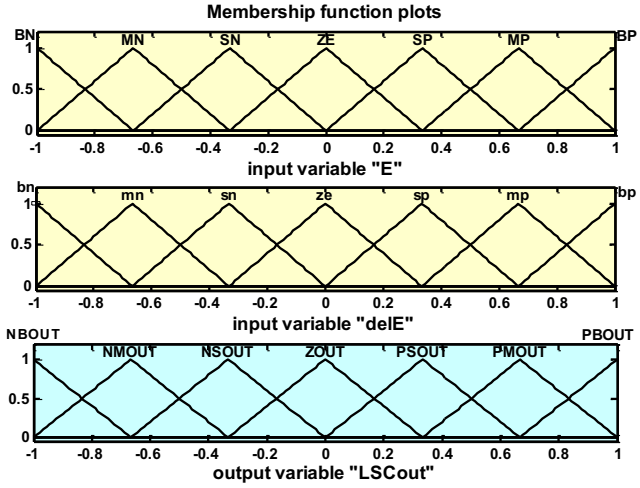

(a)

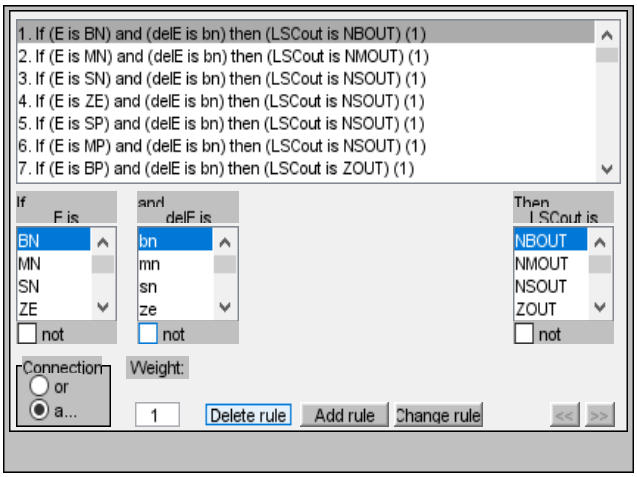

(b)

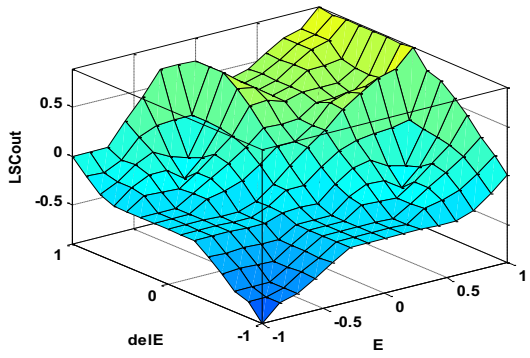

(c)

Fig. 7. (a) Membership functions for input and output variables. (b) IF-THEN Mamdani rule (c) Surface view of the IF-THEN Mamdani rule

5. Simulation results and discussions

For the purpose of analysis, it is assumed that the water discharge rate varies in between 0.4 m^3/sec and 0.9 m^3/sec as shown in Fig. 8. The proposed MHPG system is simulated in MATLAB/Simulink as shown in Fig. 9. In case of a MHPG, the water discharge rate can attain a minimum value of 0.2 m^3/sec [32]. Under this condition, the waveforms of the frequency, speed and the RMS voltage of the generator are observed. The minimum generator speed is found to be 1430 RPM with a frequency of 47.6 Hz and generated rms voltage of 360V corresponding to the minimum water discharge rate of 0.4 m^3/sec. fed to the load or grid due to poor power quality of the generation. Hence, it is necessary to regulate the output parameters with the permissible limits. Therefore, it is proposed to implement AC-DC-AC converter which is of active front end type to improve the power quality of the system so that it can be connected to the load or a grid.

The simulation results for two cases of resistive and inductive loads are presented at sub-sections Case-I and Case-II respectively. The performance analysis for each cases are carried out for both conventional PI control based system and fuzzy PI control based system. The effects of variations in modulation index and switching frequency are first studied for both PI and Fuzzy PI controller based converters. The switching frequencies are varied in the range of 1 kHz to 5 kHz and that of the modulation indices from 0.5 to 1.4. The effects of these variations are analysed in both the generator (CAG-1 and CAG-2) voltages and the load voltage. The %THD of the CAG-1 voltage is found to be improved with Fuzzy PI based converter compared to

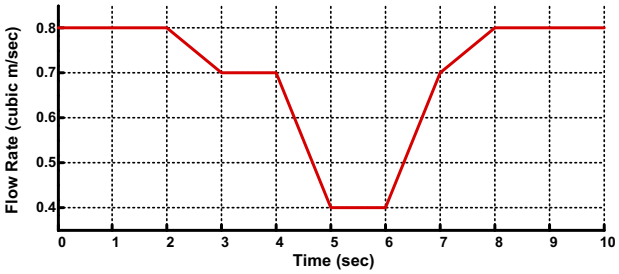

(a)

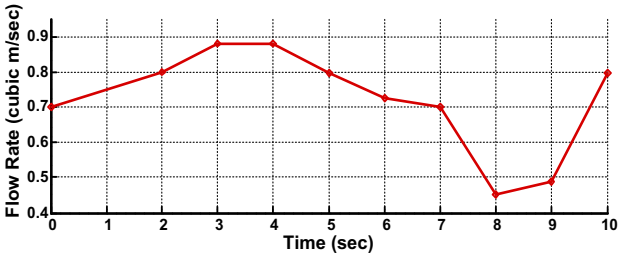

(b)

Fig. 8. Profile of variable flow rate for (a) variable turbine-1 and (b) variable turbine-2.

that of PI based converter in all the cases as shown in Fig. 10. However, the %THD values are found to be minimum for the switching frequency of 2 kHz. For lower switching frequency of 1 kHz, the %THD values seem to be better at low modulation index but for 2 kHz and 5 kHz, the values seem to be rather decreasing and maintained at certain value. Similar observations are also found in the cases of CAG-2 voltage and the load voltage as shown in Fig. 11 and Fig. 12 respectively. Hence, on an average the results at switching frequency of 2 kHz and modulation index of 1 give better performance compared to other combinations. The detail analysis of the result at switching frequency of 2

kHz and modulation index of 1 is presented in the subsequent sections.

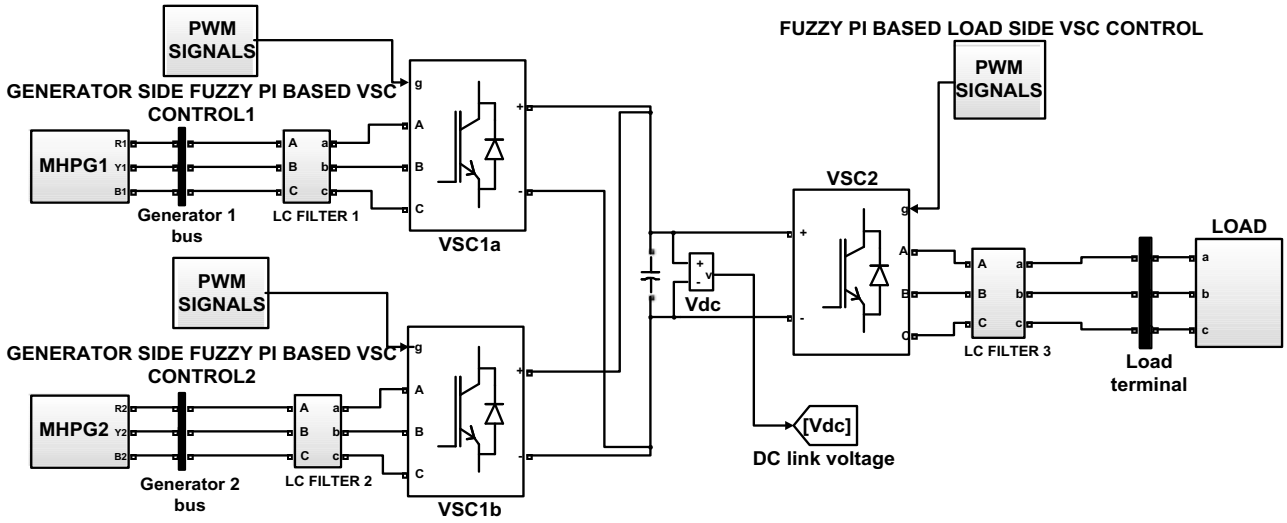

Fig. 9. Simulink block diagram of an isolated MHPG system with active front end AC-DC-AC converter.

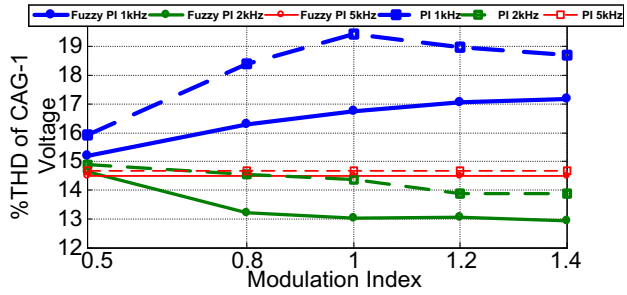

Fig. 10. Variation in %THD of CAG-1 Voltage with variation in modulation index

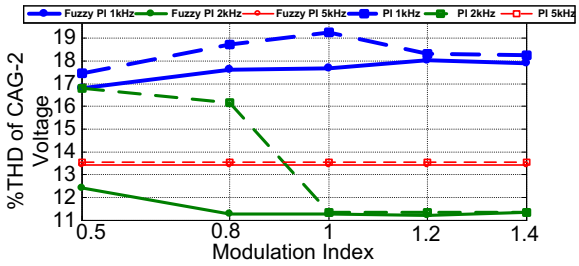

Fig. 11. Variation in %THD of CAG-2 Voltage with variation in modulation index

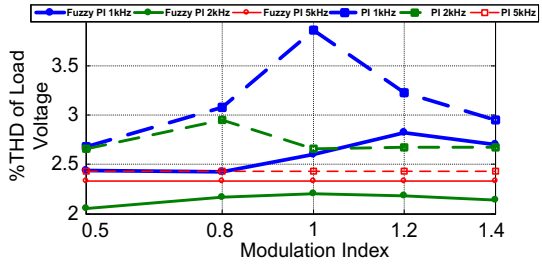

Fig. 12. Variation in %THD of load voltage with variation in modulation index

Case I: A 9 kW balanced three phase resistive load is connected at 3.5 sec and withdrawn at 7 sec

In this case, both the conventional PI based and Fuzzy PI based systems give stable and satisfactory results. The performance comparison is presented on four basic parameters. Firstly, the output waveforms of the frequencies taken at generator bus, load bus and the speeds of the two generators are observed as shown in Figs. 13 and 14. As the turbines of the two generators are considered to be variable, the corresponding variations in the speeds and frequencies are seen at each of the generator buses. Despites these varying frequencies, the output frequency is found to be constant at the rated frequency of 50 Hz, in both the cases. However, during loading, the output frequency of the Fuzzy PI based system is found to be much smoother compared to that of the conventional PI based system.

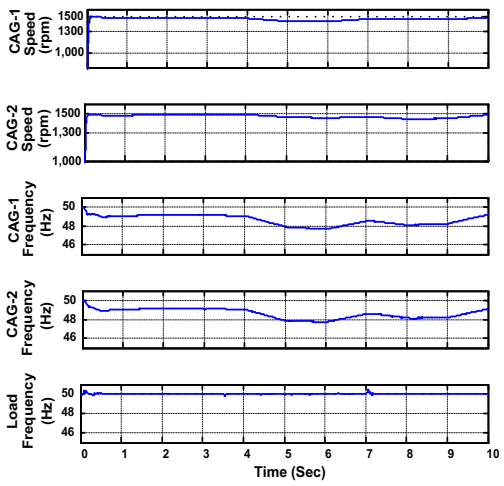

Fig. 13. Profiles of Speeds and Frequencies resistive load of 9 kW with PI control.

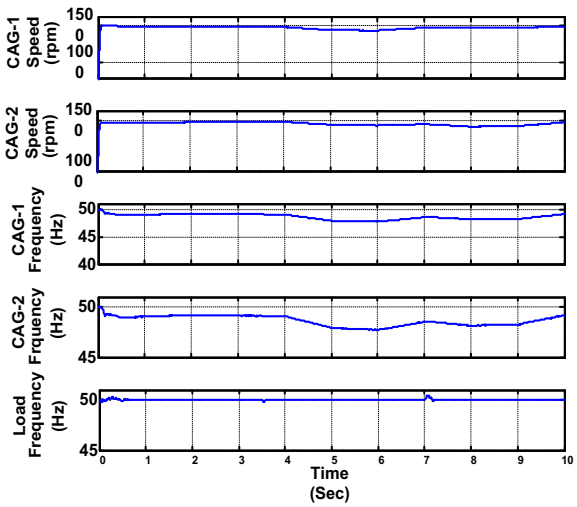

Fig. 14. Profiles of Speeds and Frequencies resistive load of 9 kW with fuzzy PI control

The voltages profiles are shown in Figs. 15 and 16. The varying peaks are visible from the generator voltages due to variable inputs in cases of CAGs voltages. The load voltage and the dc link voltage are maintained. The load voltage shows slight sagging at 227.41 V rms during the period while it found to be improved with fuzzy PI control at 244.02 V rms as shown in Figs. 15 and 16 respectively.

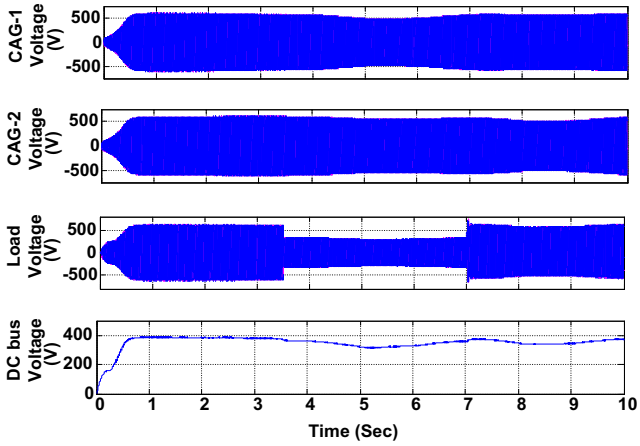

Fig. 15. Voltage profiles at different buses for resistive load of 9 kW with PI control.

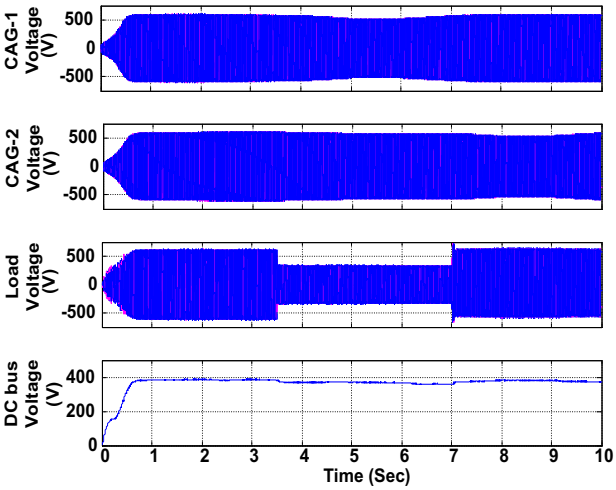

Fig. 16. Voltage profiles at different buses for resistive load of 9 kW with fuzzy PI control.

As depicted from the power curves in Figs. 17 and 18, the power consumptions are found to be optimum with peak load current of 20 A.

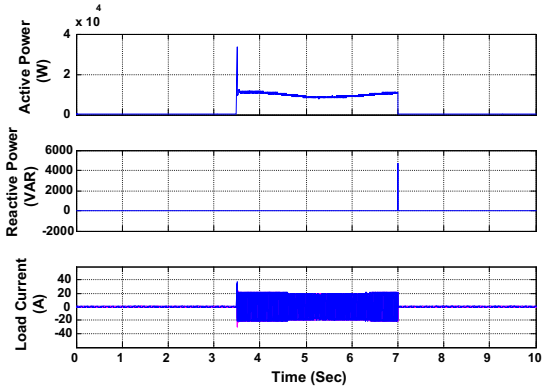

Fig. 17. Waveforms for Powers and Load Current for R-load of 9 kW with PI control.

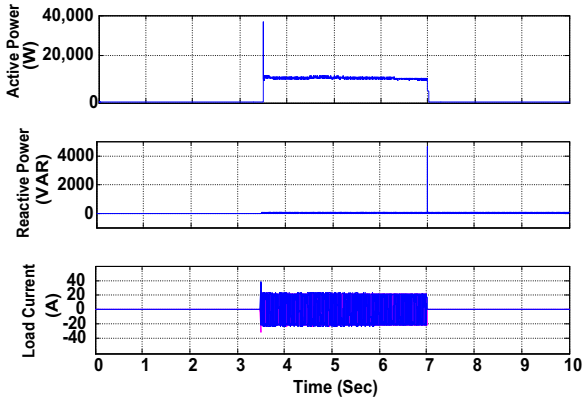

Fig. 18. Waveforms for Powers and Load Current for R-load of 9kW with fuzzy PI control.

The FFT analysis of voltage waveforms at generator buses and load buses are studied as shown in Figs. 19, 20, 21, 22, 23 and 24. It is found that there are slight improvement in the %THD of CAGs voltages with fuzzy PI control. The load voltage % THD is found to be improving with fuzzy PI control at 2.2% against 2.65% with conventional PI control. In Fig. 25, the analysis of total demand distortion (TDD) of the load current is carried out

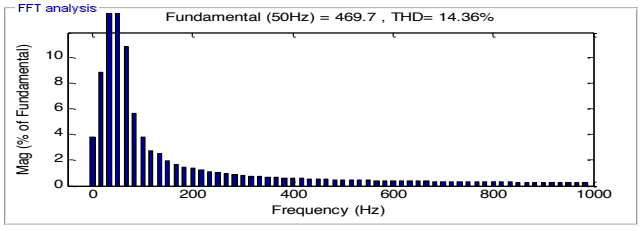

Fig. 19. FFT Analysis of CAG-1 Voltage for R-load of 9 kW.

for harmonic order upto 20th. The analysis result shows that the two controllers give almost same values with %TDD values of 1.94% each.

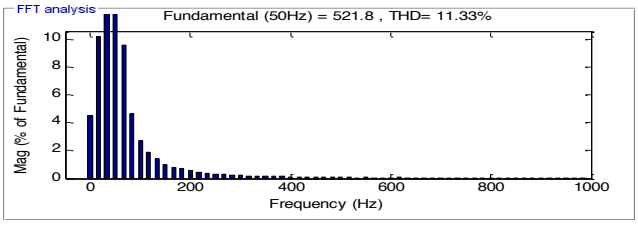

Fig. 20. FFT Analysis of CAG-2 Voltage for R-load of 9 kW.

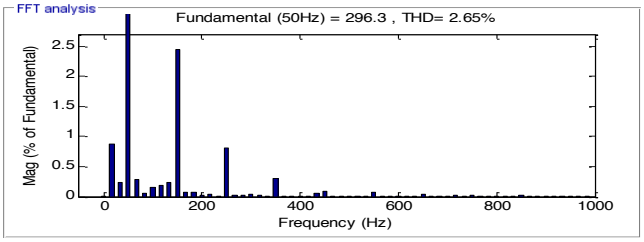

Fig. 21. FFT Analysis of Load Voltage for R-load of 9 kW.

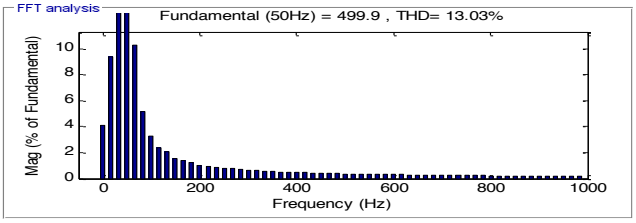

Fig. 22. CAG-1 Voltage FFT Analysis or resistive load of 9 kW with fuzzy PI control.

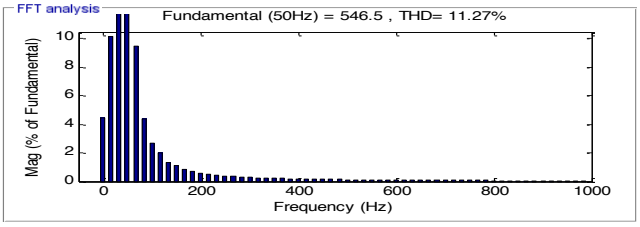

Fig. 23. CAG-2 Voltage FFT Analysis or resistive load of 9 kW with fuzzy PI control.

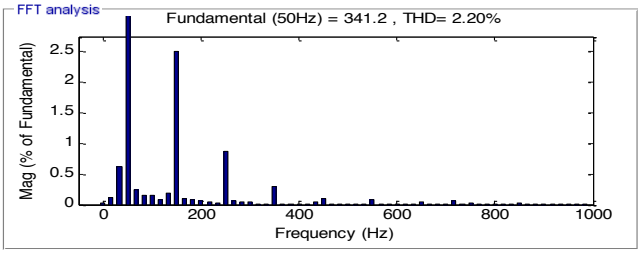

Fig. 24. Load Voltage FFT Analysis or resistive load of 9 kW with fuzzy PI control.

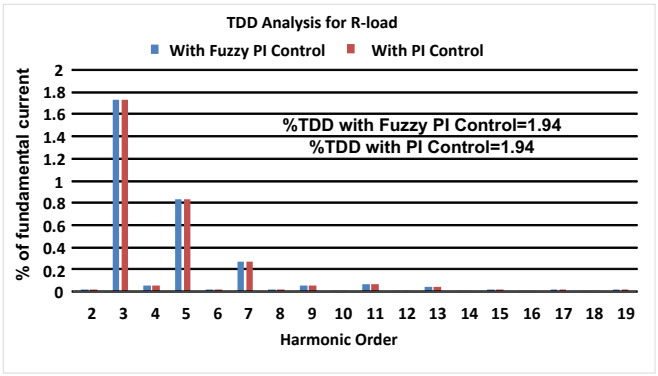

Fig. 25. Comparison of %TDD of Load Current for R load of 9 kW

Case II: A 5 kW and 4 kVAR balanced load of inductive type is loaded at 3.5 sec and withdrawn at 8.5 sec.

In this case, the results are obtained as in the first case which also varying generated frequencies and controlled or constant output. As seen from the results, the Fuzzy PI based system shows slightly better load frequency profile as compared to conventional PI, as in the case of resistive loading. However, the load frequency is well maintained at rated value in both the cases as shown in Figs. 26 & 27.

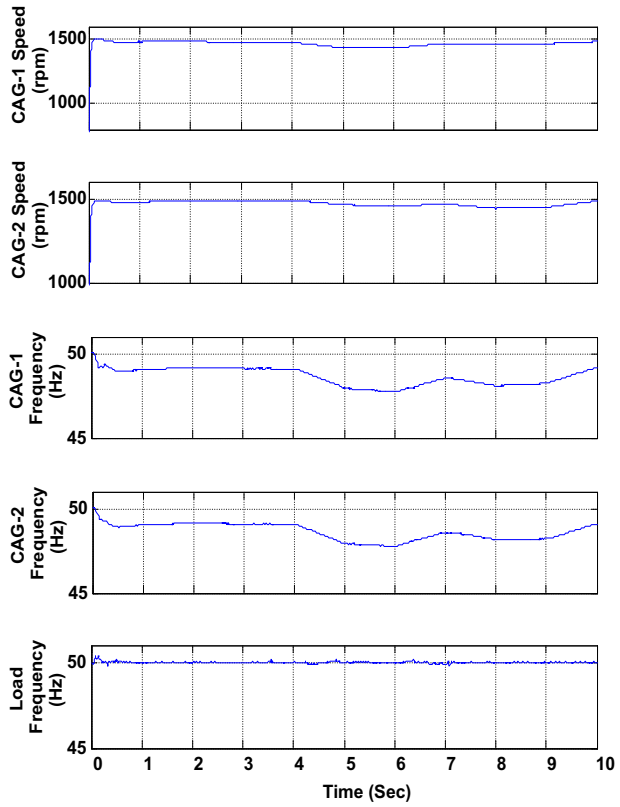

Fig. 26. Generators speed and frequencies for inductive load with PI control.

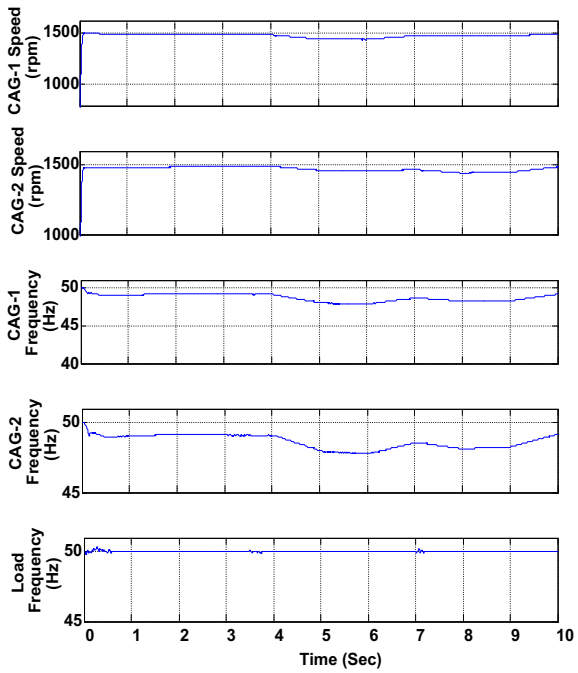

Fig. 27. Waveforms of resultant frequencies and speed for Case I with Fuzzy PI controller

The load voltage and dc link voltage are also found to be maintained under the same conditions of varying generator speeds as shown in Figs. 28 and 29. The load voltages sag during loading at an rms value of about 252.70 V rms with conventional PI control whereas it is found to be improved at 274.98 V rms with that of fuzzy PI control. The problem of voltage sagging can be eliminated with the help of a compensator. The varying peaks are visible from the generator voltages due to variable inputs in cases of CAGs voltages just as in the first case. The load voltage and the dc link voltage are found to be maintained.

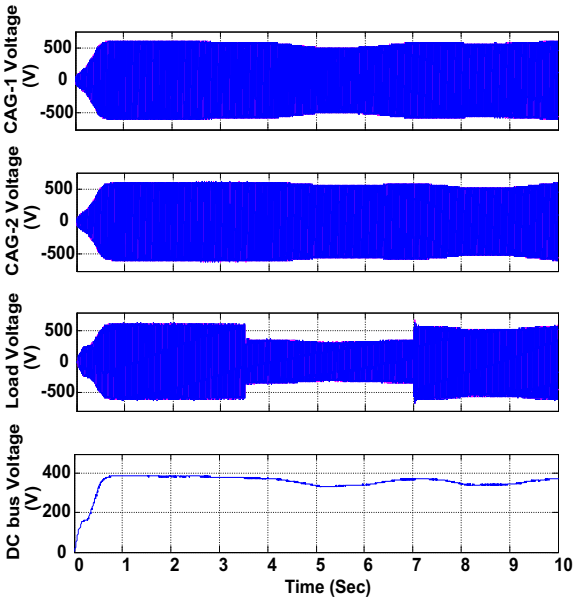

Fig. 28. Resultant voltage profiles at various buses for Case I with conventional PI controller.

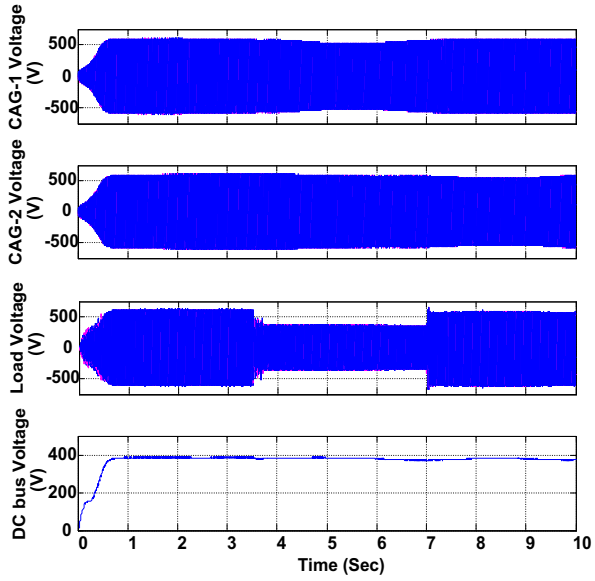

Fig. 29. Voltage profiles for inductive load with fuzzy PI control.

The power consumptions are optimum as can be seen from the results shown in Figs. 30 & 31. The peak load currents in both the cases are found to be about 20 A.

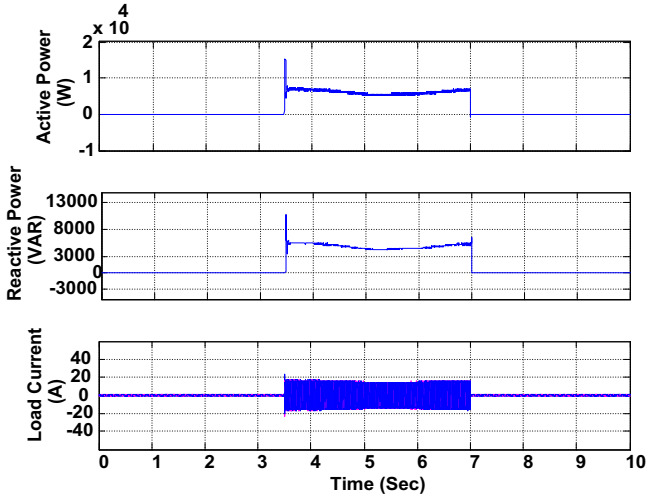

Fig. 30. Power consumption profiles along with load current for inductive load with PI control.

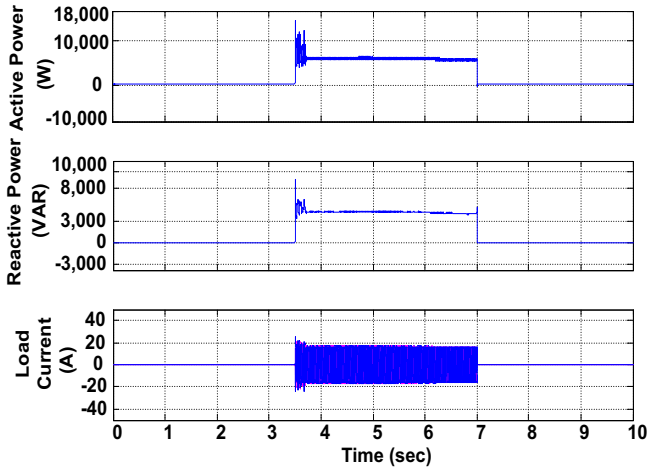

Fig. 31. Power consumption profiles along with load current for inductive load with fuzzy PI control.

The %THD's of the voltage waveforms at generator bus and load bus are considered for both the types of controllers. The results are shown in Figs. 32, 33, 34, 35, 36 and 37. As in the first case, the %THDs are slightly improved in the generator buses whereas in the load voltage it is found to be 2.97 with conventional PI control and 2.70 with fuzzy PI control. In Fig. 38, the analysis of total demand distortion (TDD) of the load current is carried out upto 20th harmonic order. Unlike the first case, the analysis result shows that the Fuzzy PI based controller gives better %TDD value of 0.97% compared to that of conventional PI controller which gives 1.94%.

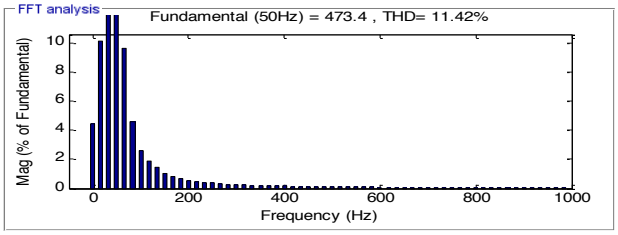

Fig. 32. FFT Analysis of CAG-1 Voltage for RL load of 5 kW and 4 kVAR with conventional PI control.

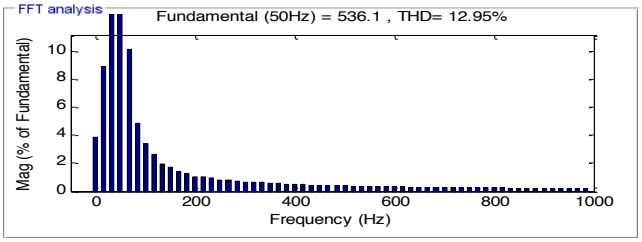

Fig. 33. FFT Analysis of CAG-2 Voltage for RL load of 5 kW and 4 kVAR with conventional PI control.

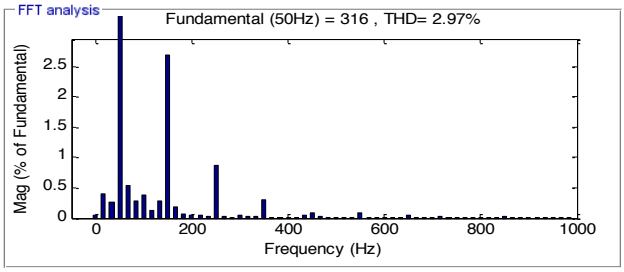

Fig. 34. FFT Analysis of Load Voltage for RL load of 5 kW and 4 kVAR with conventional PI control.

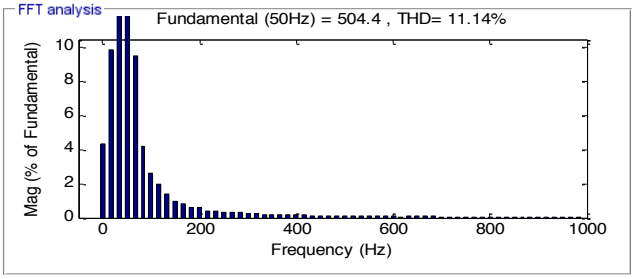

Fig. 35. FFT Analysis of CAG-1 Voltage for RL load of 5 kW and 4 kVAR with fuzzy PI control.

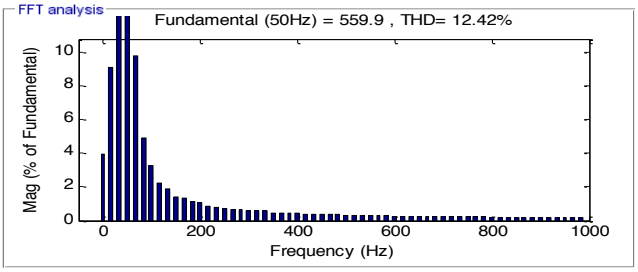

Fig. 36. FFT Analysis of CAG-2 Voltage for RL load of 5 kW and 4 kVAR with fuzzy PI control.

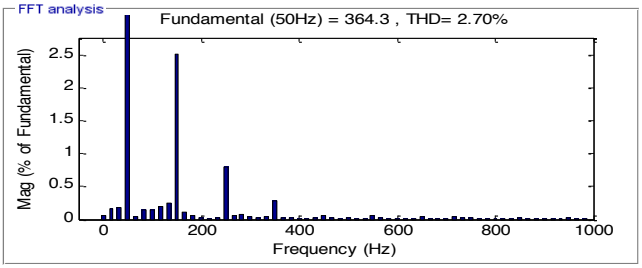

Fig. 37. FFT Analysis of Load Voltage for RL load of 5 kW and 4 kVAR with fuzzy PI control.

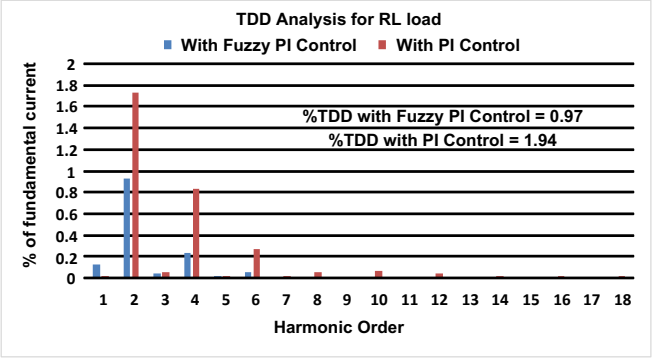

Fig. 38. Comparison of %TDD of Load Current for RL load of 5 kW and 4 kVar

The summarized results with performance comparison is given in Table 2 below.

Table 2. Performance comparison of PI and Fuzzy PI based system on loading

Load	Control ler	Performance Parameters with PI Control							
		Frequency (Hz)			*RMS Load Voltage (V)*	*%THD*			*%TDD*
		CAG #1	*CAG #2*	*Load*		*CAG-1 Voltage*	*CAG-2 Voltage*	*V load*	*I load*
R	PI	Variable		50	227.41	14.36	11.33	2.65	1.94
	Fuzzy PI	Variable		50	252.70	13.03	11.27	2.20	1.94
RL	PI	Variable		50	244.02	11.42	12.95	2.97	1.94
	Fuzzy PI	Variable		50	274.98	11.14	12.42	2.70	0.97

6. Conclusion

This paper presents a new MHPG scheme which is feasible and convenient to generate electricity for a remote area. The proposed scheme is realized by implementing an active front end AC-DC-AC converter and is able to generate and supply quality power from variable water flow to feed remote areas. In the performance analysis, the proposed model with Fuzzy PI based system is found to perform better than that of a conventional PI controlled system. The optimum operating point is initially found out in terms of switching frequency and modulation index. It is found that the system with 2 kHz switching frequency and modulation index closed to 1 gives better result. Under this condition, the Fuzzy PI based MHPG system gives better performances in terms of improved output voltage, frequency, %THD's, %TDD's and dc link voltage profile as summarised in Table 2. The load side harmonics are found to be well within permissible limits as prescribed by IEEE standards [34]. The generator side harmonics are observed to be present as the study considers variable turbine input but effort has been made to reduce the same and it is found to be reduced more in the case of Fuzzy PI based system. Also, the output frequencies are maintained constant in both the cases of resistive and inductive loads and the requirement of frequency controller is dispensed with. Though the voltages profiles are well maintained, there are slight sagging in the load voltages during loading which can be either eliminated by voltage compensator or re-designing of the DC-link capacitor with improved control algorithm. Since, the scheme considers full back to back converter, the converter has to carry the full load current of the system and hence, the scheme is suitable only for small scale MHPG. Overall, the proposed MHPG system gives a superior performance with Fuzzy PI controller as evident from the results of the simulation.

References

[1] IEA, 2018. Available at https://www.iea.org/weo2018/

[2] Renewables 2019, Global Status Reports. Available at https://www.ren21.net/wp-content/uploads/2019/05/gsr_2019_full_report_en.pdf

[3] CEA, 2018. Available at http://www.cea.nic.in/reports/committee/nep/nep_jan_2018.pdf

[4] S. Nababan, E. Muljadi, and F. Blaabjerg, "An overview of power topologies for micro-hydro turbines," Proc. - 2012 3rd IEEE Int. Symp. Power Electron. Distrib. Gener. Syst. PEDG 2012, pp. 737–744, 2012.

[5] Ofualagba, G, and U. E.U, "The Analysis and Modelling of a Self-excited Induction Generator Driven by a Variable Speed Wind Turbine," Fundam. Adv. Top. Wind Power, pp. 249–268, 2011, ch.11.

[6] Z. Alnasir and M. Kazerani, "Performance comparison of standalone SCIG and PMSG-based wind energy conversion systems," *Can. Conf. Electr. Comput. Eng.*, pp. 1–8, 2014.

[7] S. Hazra and P. S. Sensarma, "Self-excitation and control of an induction generator in a stand-alone wind energy conversion system," IET Renew. Power Gener., vol. 4, no. 4, pp. 383–393, 2010.

[8] M. G. Simões, B. K. Bose, and R. J. Spiegel, "Fuzzy logic based intelligent control of a variable speed cage machine wind generation system," IEEE Trans. Power Electron., vol. 12, no. 1, pp. 87–95, 1997.

[9] N. Harrabi, M. Souissi, A. Aitouche, and M. Chaabane, "Intelligent control of grid-connected AC-DC- AC converters for a WECS based on T-S fuzzy interconnected systems modelling," IET Power Electron., vol. 11, no. 9, pp. 1507–1518, 2018.

[10] T. Ahmed, E. Hiraki, M. Nakaoka, and O. Noro, "Three-Phase Self-Excited Induction Generator Driven by Variable-Speed Prime Mover for Clean Renewable Energy Utilizations and Its Terminal Voltage Regulation Characteristics by Static VAR Compensator," Conf. Rec. - IAS Annu. Meet. (IEEE Ind. Appl. Soc., vol. 2, pp. 693–700, 2003.

[11] S. Zouggar, Y. Zidani, M. L. Elhafyani, T. Ouchbel, M. Seddik, and M. Oukili, "Neural control of the self-excited induction generator for variable-speed wind turbine generation," Smart Innov. Syst. Technol., vol. 12, pp. 213–223, 2012.

[12] E. Kabalcı, E. Irmak, I. Çolak, "Design of an AC-DC-AC converter for wind turbines", International Journal of Energy Research, Wiley Interscience, DOI: 10.1002/er.1770, Vol. 36, No. 2, pp. 169-175.

[13] N. Harrabi, M. Souissi, A. Aitouche, and M. Chaabane, "Control of a DC-AC inverter in a wind energy generation system using T-S fuzzy modeling," Conf. Control Fault-Tolerant Syst. SysTol, vol. 2016-November, pp. 660–665, 2016.

[14] M. Quraan, Q. Farhat, and M. Bornat, "A new control scheme of back-to-back converter for wind energy technology," 2017 6th Int. Conf. Renew. Energy Res. Appl. ICRERA 2017, vol. 2017-January, pp. 354–358, 2017.

[15] T. Barisa, D. Sumina, and M. Kutija, "Control of generator-and grid-side converter for the interior permanent magnet synchronous generator," *2015 Int. Conf. Renew. Energy Res. Appl. ICRERA 2015*, pp. 1015–1020, 2015.

[16] Watson, D. B., and I. P. Milner. "Autonomous and Parallel Operation of Self-Excited Induction Generators." The International Journal of Electrical Engineering & Education, vol. 22, no. 4, Oct. 1985, pp. 365–374.

[17] C. Lee and L. Wang, "Self-Excited Induction Genepmtors," IEEE Transactions on Energy Conversion, vol. 13, no. 2, pp. 117-123, June 1998.

[18] A. H. Al-Bahrani and N. H. Malik, "Parallel Operation of Self-Excited Induction Generators," J. King Saud Univ. - Eng. Sci., vol. 6, no. 1, pp. 79–96, 1994.

[19] C. Chakraborty, M. Ishida, S. N. Bhadra, and A. K. Chattopadhyay, "Performance of parallel-operated self-excited induction generators with the variation of machine parameters," Proc. Int. Conf. Power Electron. Drive Syst., vol. 1, no. July, pp. 86–91, 1999.

[20] B. Singh and G. K. Kasal, "Independent voltage and frequency controller for a parallel operated isolated three-phase asynchronous generators," Eur. Trans. Electr. Power, vol. 19, no. 6, pp. 839–853, Sep. 2009.

[21] C. P. Ion and C. Marinescu, "Control of parallel operating micro hydro power plants," Proc. Int. Conf. Optim. Electr. Electron. Equipment, OPTIM, pp. 1204–1209, 2010.

[22] M. H. Baloch, J. Wang, and G. S. Kaloi, "A review of the state of the art control techniques for wind energy conversion system," Int. J. Renew. Energy Res., vol. 6, no. 4, pp. 1277–1295, 2016.

[23] A. G. Aissaoui, A. Tahour, M. Abid, N. Essounbouli, and F. Nollet, "Using Neuro Fuzzy PI techniques in wind turbine control," Proc. 2013 Int. Conf. Renew. Energy Res. Appl. ICRERA 2013, no. October, pp. 605–610, 2013.

[24] K. Belmokhtar, M. L. Doumbia, and K. Agbossou, "Modelling and fuzzy logic control of DFIG based Wind Energy Conversion Systems," IEEE Int. Symp. Ind. Electron., pp. 1888–1893, 2012.

[25] S. A. Deraz and F. E. Abdel Kader, "A new control strategy for a stand-alone self-excited induction generator driven by a variable speed wind turbine," Renew. Energy, vol. 51, pp. 263–273, 2013.

[26] F. J. Lin, P. K. Huang, C. C. Wang, and L. T. Teng, "An induction generator system using fuzzy modeling and recurrent fuzzy neural network," IEEE Trans. Power Electron., vol. 22, no. 1, pp. 260–271, 2007.

[27] J. Osmic, M. Kusljugic, and A. Mujcinagic, "Fuzzy controller for inertial support of variable speed wind generator," IET Conf. Publ., vol. 2016, no. CP711, pp. 1–8, 2016.

[28] D. Sindhu and G. Irusapparajan, "Analysis of the performance of 3 phase system by using D-Q transformation and fuzzy hysteresis controller," IET Semin. Dig., vol. 2013, no. 8, pp. 240–247, 2013.

[29] C. Cecati, A. Dell'Aquila, M. Liserre, and A. Ometto, "A fuzzy-logic-based controller for active rectifier," IEEE Trans. Ind. Appl., vol. 39, no. 1, pp. 105–112, 2003.

[30] Dong-Choon Lee, and Jeong-Ik Jang, "Output voltage control of PWM inverters for stand-alone wind power generation systems using feedback linearization," Conference Record of the 2005 - IEEE Industry Applications Conference 14th IAS Annual Meeting, vol. 3, pp. 1626–1631, October 2005.

[31] A. Harrouz, K. Nourdine, K. Kayisli, H. I. Bulbul, and I. Colak, "A Fuzzy Controller for Stabilization of Asynchronous Machine," 7th Int. IEEE Conf. Renew. Energy Res. Appl. ICRERA 2018, vol. 5, pp. 1369–1373, 2018.

[32] Benyamina, S. Moulahoum, I. Colak; R. Bayindir, "Hybrid fuzzy logic-artificial neural network controller for shunt active power filter", 5th International Conference on Renewable Energy Research and Applications (ICRERA), pp.837-844, 2016

[33] P. D. Singh and S. Gao, "An Isolated Hydro Power Generation using Parallel Asynchronous Generators at Variable Turbine Inputs using AC-DC-AC Converter," 2018 8th IEEE India International Conference on Power Electronics (IICPE), JAIPUR, India, 2018, pp. 1-6.

[34] IEEE Standard 519-2014, Recommended Practices and requirements for Harmonic Control in Electric Power Systems. The Institute of Electrical and Electronics Engineers, 2014. (Standards and Reports)

Appendices

Machine Parameters:

Squirrel Case Induction Machine: 7.5 kW, 3 phase, 415 V, 14.5 A, 50 Hz, Y-Connected, 4-Pole, R_s = 0.9 Ω, R_r = 0.66 Ω, $X_{ls} = X_{lr}$ = 0.00457 H and J = 0.1384 kgm^2

Prime mover characteristics:

$T_m = \tau_0 - f(Q).\omega_r$ where, τ_0 = 1242,
f(Q) varies with varying flow rate

Generator side controller Parameters:

DC voltage regulator: K_p = 0.15, K_i = 0.0002
Current regulator: K_p = 0.6, K_i = 0.009
Load side controller Parameters:
K_p = 0.38, K_I = 0.0002

Filter Parameters:

Generator side: R=5 Ω, L = 40 mH, C = 160 μF
Load side: R=1.13 Ω, L = 22 mH, C = 300 μF

DC link Capacitor: C =1800 μF, V_{dc} = 380 V